Published in final edited form as:
Cell Rep. 2012 December 27; 2(6): 1492–1497. doi:10.1016/j.celrep.2012.11.001.

The Sirtuin 2 Inhibitor AK-7 is Neuroprotective in Huntington Disease Mouse Models

Vanita Chopra[1], **Luisa Quinti**[1], **Jinho Kim**[2], **Lorraine Vollor**[1], **Lakshminarayanan Kumaraswamy**[1], **Christina Edgerly**[2], **Patricia M. Cipicchio**[2], **Molly A. Lauver**[2], **Soo Hyuk Choi**[3], **Richard B. Silverman**[3], **Robert J. Ferrante**[2], **Steven Hersch**[1], and **Aleksey G. Kazantsev**[1,*]

[1]Department of Neurology, Harvard Medical School, Massachusetts General Hospital, Charlestown, MA, 02129-4404, USA

[2]Neurological Surgery, Neurology, and Neurobiology Departments, University of Pittsburgh, Pittsburgh, PA 15213, USA and the Geriatric Research Educational and Clinical Center (00-GR-H), V.A. Pittsburgh Healthcare System, 7180 Highland Drive, Pittsburgh, PA 15206, USA

[3]Department of Chemistry, Department of Molecular Bioscience, Chemistry of Life Processes Institute, Center for Molecular Innovation and Drug Discovery, Northwestern University, Evanston, Il 60208-3113, USA

Summary

Inhibition of sirtuin 2 deacetylase mediates protective effects in cell and invertebrate models of Parkinson's disease and Huntington's disease (HD). Here we report the *in vivo* efficacy of a brain-permeable sirtuin 2 inhibitor in two genetic mouse models of HD. Compound treatment resulted in improved motor function, extended survival, and reduced brain atrophy and is associated with marked reduction of aggregated mutant huntingtin, a hallmark of HD pathology. Our results provide preclinical validation of SIRT2 inhibition as a potential therapeutic target for HD and support the further development of SIRT2 inhibitors for testing in humans.

Introduction

Huntington's disease (HD) is an autosomal dominant monogenetic neurodegenerative disorder, characterized by progressive neuronal loss, motor dysfunction, emotional disturbances, dementia, weight loss, and premature death (Young, 2003). HD is caused by an expansion of CAG-triplet repeats within exon 1 of the HD gene, which is translated into mutant huntingtin protein with pathologically extended polyglutamines prone to misfolding and aggregation (The Huntington's Disease Collaborative Research Group, 1993). Although huntingtin, a predominantly cytoplasmic protein of uncertain function, is ubiquitously

*To whom correspondence should be addressed: Aleksey G. Kazantsev, PhD, Associate Professor in Neurology, Harvard Medical School, Drug Discovery Laboratory, MassGeneral Institute for Neurodegenerative Disease Massachusetts, General Hospital Building 114-3300 16th Street Charlestown, MA, 02129-4404, Tel: 617-726-1274, fax: 617-724-1480, akazantsev@partners.org.

Author contributions: AK, SH, VC, RJF, and RBS designed the research; VC, LQ, LV, LN, JK, CE, PC, and SHC performed research; VC, LQ, RJF analyzed data; AK, VC, SH, RJF, and RBS wrote the paper.

Conflict of interest statement: The authors declare no competing financial interests.

expressed in the body and brain, the earliest neuropathological changes are found in the neostriatum and cerebral cortex (Rosas et al., 2008). Intracellular aggregates, containing misfolded huntingtin, can be readily detected in brain both presymptomatically and throughout the course of the disease, however, the role for polyglutamine aggregation in neurodegeneration has not been resolved (Truant et al., 2008). It has become evident that mutant huntingtin perturbs multiple biochemical pathways; however, no dominant neurodegenerative mechanism has emerged (Hersch and Rosas, 2008). Although preclinical studies in HD mouse models have identified candidate therapeutics, there is not yet a neuroprotective therapy demonstrated to slow or halt disease progression in human HD.

The sirtuin family, which includes seven mammalian NAD^+-dependent enzymes (SIRT1-SIRT7), has received much attention in recent years due to their diverse physiological functions in metabolism, aging, and age-related human diseases (Donmez and Guarente, 2010). The second family member, sirtuin 2 (SIRT2), acts as a NAD^+-dependent deacetylase on a variety of histone and non-histone substrates, including a major component of microtubules, α-tubulin (North et al., 2003; Vaquero et al., 2006). SIRT2 is a highly abundant protein in the adult brain, where an alternatively spliced isoform, SIRT2.2, is preferentially expressed (Maxwell et al., 2011). In the brain, SIRT2 expression is detected in oligodendrocytes (Beirowski et al., 2011; Ji et al., 2011) and neurons (Luthi-Carter et al., 2010; Maxwell et al., 2011), although the protein function(s) remain elusive. In previous studies genetic or pharmacological inhibition of SIRT2 in primary neuronal and invertebrate animal models of Parkinson's disease and HD rescued neurotoxicity mediated by the causative α-synuclein and huntingtin (Htt) proteins (Luthi-Carter et al., 2010; Outeiro et al., 2007; Pallos et al., 2008). In primary neuronal HD models, inhibition of SIRT2 reduces mutant huntingtin aggregates, and, in part, the neuroprotection was achieved by transcriptional repression of cholesterol biosynthesis (Luthi-Carter et al., 2010). Conversely, constitutive genetic inhibition in HD transgenic mice was not neuroprotective and did not affect polyglutamine aggregation (Bobrowska et al., 2012). In addition, a null SIRT2 genetic background or acute pharmacological inhibition did not affect transcriptional expression of cholesterol biosynthesis enzymes in the R6/2 HD mouse model (Bobrowska et al., 2012).

Here we utilized several preclinical target validation paradigms and examined the *in vivo* efficacy of SIRT2 inhibition in HD mouse models, using chronic pharmacological treatment. We took advantage of a recently developed brain-permeable selective SIRT2 inhibitor 3-(1-azepanylsulfonyl)-N-(3-bromphenyl) benzamide (AK-7) (Taylor et al., 2011), which is neuroprotective *in vitro* and reduces polyglutamine inclusions and cholesterol levels in neurons. Despite sub-optimal pharmacological properties, AK-7 mediated neuroprotection *in vitro* was achieved at doses comparable with brain concentrations in wild-type and HD mice, followed by acute treatment (Taylor et al., 2011). These results prompted us to examine the *in vivo* efficacy of AK-7 using two well-characterized genetic mouse models of HD.

Mouse models of HD, recapitulating key pathological features, have been developed and successfully used for preclinical testing of therapeutics that have proceeded to clinical trials. For this study we employed the widely studied R6/2 mouse model, where expression of multiple mutant exon 1 Htt fragments with ~150CAG repeats results in a robust neurological phenotype and premature death at approximately 100 days of age (Stack et al., 2005). We also used the more genetically accurate 140CAG full-length Htt knock-in model, which manifests a mild neurological phenotype and has a normal life span (Menalled et al., 2003). Using comprehensive outcome measures to assess efficacy, we demonstrate that chronic treatment with brain-permeable SIRT2 inhibitor AK-7 resulted in improved motor function, extended survival, and reduced brain atrophy in HD mice. Furthermore, the treatment benefits are associated with significant reduction of mutant huntingtin aggregates in HD

brain. Our study strongly advances the preclinical validation of SIRT2 inhibition as a neuroprotection target for HD. It also provides a rationale for the development of SIRT2 inhibitors with improved pharmacological properties that could be advanced to human clinical trials.

Results

Design of AK-7 drug trials in HD mouse models

First, we assessed the efficacy of AK-7 treatment in the R6/2 mouse model. The comparative analysis and quantification of the expression levels of SIRT2 isoforms in cortical tissues of R6/2 mice as well as knock-in HD mice by Western analysis showed their clear presence in target tissue (Figure S1). There were no progressive changes detected in SIRT2 levels in R6/2 or 140CAG mice as they age, suggesting that the levels of SIRT2 were not modified by disease. The compound synthesis scheme for the study is shown in (Figure S2). In the acute toxicity studies, the compound was safe up to 2500 mg/kg as no mortality was observed up to this dose. For chronic drug-treatment doses of 10, 20, and 30 mg/kg were selected to assess AK-7 efficacy in the phenotypic study. Given the limited brain metabolic stability of AK-7 (half-life ~2 h) (Taylor et al., 2011), the compound and vehicle control treated-mice were administered by i.p. injections twice daily. The 20 mg/kg dose was used for neuropathological and biochemical studies once phenotypic benefits were detected in both models at that dose. Treatment was initiated in mice at 4 weeks of age and continued up to 14 weeks or otherwise specified.

AK-7 improves the behavior and neuropathological phenotype and extends survival of R6/2 HD mice

AK-7 treated R6/2 mice performed significantly better than vehicle treated littermates on the accelerating rotarod at 8 and 11 weeks of age (Figure 1A). Latency to fall was increased by 29% at 8 weeks of age with AK-7 treatment at the 10mg/kg dose and by 44% at 11 weeks of age with AK-7 treatment at 10 and 20 mg/kg doses. Values were significant only at the age of 11 weeks.

AK-7 at the 10mg/kg dose was also effective in extending the survival of R6/2 mice (Figure 1B). Mean survival of placebo treated R6/2 mice was 94.8±5.4, as compared with 109.2± 2.6 in AK-7 treated (10mg/kg) mice; mean survival of treated R6/2 mice was increased by 13.2% (Figure 1C). At the 20 mg/kg dose, treatment with AK-7 caused a non-significant trend towards survival extension. No effect of the 30mg/kg dose on survival was observed, possibly due to systemic toxicity at this high dose.

AK-7 ameliorates HD neuropathology in R6/2 mice

To assess the biological effects of AK-7 on neuropathology, mice treated with 20mg/kg of AK-7, were sacrificed at 12-weeks of age. We selected the highest tolerable dose (20 mg/kg) for which there was evidence of clinical efficacy in both models to examine effects on neuropathology in brain. Unbiased stereological methods were used to measure the striatal and neuronal atrophy. The morphometric analysis showed a small but statistically significant improvement in both total striatal volume and striatal neuronal volume (Figure 1D–F), which were increased by 9% and 15%, respectively, confirming the neuroprotective effects of AK-7 treatment. The average volume of striatal neuronal cell bodies in wild-type mice was 640 ± 22.57μm^3, as compared with 410 ± 21.6 μm^3 in 12-week-old R6/2 mice. AK-7-treated (20 mg/kg) R6/2 mice had a mean striatal neuronal cell body volume of 470 ± 10.03 μm^3, which was significantly greater than placebo-treated R6/2 control mice.

AK-7 reduces the polyglutamine aggregation in R6/2 brain

In the previous *in vitro* studies, inhibition of SIRT2 has been demonstrated to reduce mutant huntingtin aggregates, and, in part, the neuroprotection was achieved by transcriptional repression of cholesterol biosynthesis. Here, we examined the effects of AK-7 treatment on polyglutamine aggregates and cholesterol levels in R6/2 brain. Immunohistochemical analysis of the striatal sections showed a marked reduction in aggregate size in the brain of AK-7 treated HD mice (Figure 2A) and stereological quantification demonstrated a 35% reduction in aggregate volume. The mean nuclear aggregate volume in AK-7 treated mice was $8.99 \times 10^4 \pm 0.48\ \mu m^3$, as compared with $13.72 \times 10^4 \pm 0.56\ \mu m^3$ in placebo-treated R6/2 (Figure 2B). AK-7 treatment did not affect aggregate number (Figure 2C), or significantly change soluble levels of mutant Htt, measured by a highly sensitive HTRF method (Figure 2D) (Moscovitch-Lopatin et al., 2010). Nevertheless, altogether the results suggest a significant reduction of aggregated polyglutamine levels in compound-treated R6/2 brains.

Efficacy of AK-7 in 140CAG knock-in HD mice

We next assessed the effects of AK-7 treatment in the 140CAG knock-in Htt mouse model using the same dosing regimen of 10, 20, and 30 mg/kg twice daily. Treatment was started at 4 weeks of age and continued until sacrifice. We observed a significant improvement in motor activity of 140CAG mice with AK-7 treatment (Figure 3A, B). Compared to wild-type mice, there was a significant decrease in motor activity in untreated 140CAG mice as characterized by distance traveled (Figure 3A) and increase in resting time (Figure 3B), starting at 2 months through 5 months ($p<0.01$). In contrast, AK-7 treated 140CAG mice showed motor performance changes that paralleled untreated wild-type mice, with the 20 mg/kg dose being most effective and significantly different from untreated 140CAG mice ($p<0.01$). Both the 10 mg/kg and 30 mg/kg doses were only significant at 2- and 3-month treatment time intervals ($p<0.01$). The administration of AK-7 at the 20 mg/kg dose, as established in behavioral studies, markedly reduced aggregate number in the striatum of 140CAG mice at 6 months by greater than 50% (untreated 140 CAG mice: $4.31 \times 10^6 \pm 1.07$, AK-7-treated 140 CAG mice: $2.01 \times 10^6 \pm 0.63$; $p<0.01$) (Figure 3C–D). The results in this second HD mouse model demonstrate a significant reduction of aggregated polyglutamines in compound-treated brains, and correlates with the efficacy of AK-7 observed in the behavioral studies.

Discussion

In this study, treatment with AK-7 significantly improved the neurological phenotypes in both truncated and full-length HD mouse models, despite its limited potency *in vitro* and sub-optimal pharmacological properties. Remarkably, the therapeutic benefits were seen across outcome measures and included improvement of motor behavior, extension of survival, and neuroprotection, particularly in the more fulminant R6/2 disease model, where pathology is driven by the expression of six transgenes and in which the truncated mutant huntingtin aggregates quite avidly. Three compound doses, 10, 20, and 30mg/kg, were tested in both mouse models prior an analysis of neuropathological sequelae. Both the 10mg/kg and 20mg/kg doses were effective in improving motor performance and survival in the R6/2 mice. The 20mg/kg dose was found most efficacious in the behavioral studies in 140CAG knock-in mice, while 10 and 30 mg/kg doses were less effective in this model. Effects on neuropathology were assessed in mice treated with 20mg/kg, the highest tolerated dose in which there was clinical evidence for efficacy in both models. The significant improvement of neuropathology, correlated with a 35% reduction in inclusion volumes, was observed in R6/2 mice, albeit lower doses may be better tolerated in this mouse model. Notably, the AK-7 reduction of inclusion volumes in the R6/2 brain compares similarly to the effects of

the neuroprotective aggregation inhibitor C2-8 (Chopra et al., 2007). Intriguingly, selective SIRT2 inhibition activity *in vitro* has been shown for C2-8 or its structural analogs (Taylor et al., 2011), suggesting a SIRT2 inhibition-dependent neuroprotective mechanism for this compound or its metabolites. In 140CAG mice the effects of AK-7 on aggregation was even more robust, leading to reduction of inclusion numbers by 50%, and is consistent with the genetic and pharmacological properties of SIRT2 inhibition observed in *in vitro* HD neurons (Luthi-Carter et al., 2010; Taylor et al., 2011). Altogether the data from both mouse models demonstrate a correlation between animal behavioral efficacy and improved neuronal health and the reduced presence of aggregated polyglutamines in the HD brain, which likely represents a proximal mechanism of neuroprotection. Since AK-7 treatment was beneficial in two HD mouse models, the data also suggests the therapeutic potential of sulfobenzoic acid derivatives in humans. To develop more potent SIRT2 inhibitors with superior pharmacological properties, we plan to repurpose a previously identified sub-scaffold (C2-8) for bioactive sulfobenzoic acid derivatives (Choi et al., 2012).

The role of SIRT2 as a potential therapeutic target for HD has been recently investigated by analysis of F1 progeny from the genetic cross of R6/2 and SIRT2 KO mouse strains (Bobrowska et al., 2012). In contrast to our results, that study showed no apparent benefits of SIRT2 negative background on HD pathology, including loss of body weight, deficiency in motor-performance, or aggregation. The study also revealed no detectable phenotype in SIRT2 KO mice. Genetic knockouts remove target(s) from known and unknown protein complexes, disrupt target-specific signaling pathways, cause structural reshuffling, and often result in embryonic lethality or in a lack of phenotype (Barbaric et al., 2007). This is fundamentally different than gene silencing due to the transient action of small molecule drugs, which are typically rapidly disengaged from the target and degraded, leaving the target proteins intact. It is clear that a discrepant outcome from genetic and pharmacological manipulations is not limited to SIRT2. For example, no improvement of neurological phenotype has been observed in F1 progeny from the genetic cross of R6/2 and heterozygote HDAC3 knockout mice (Moumne et al., 2012). In contrast, the benefits of treating R6/2 mice with dual HDAC1/3 inhibitors have been achieved by preferentially targeting HDAC3 (Jia et al., 2012; Jia et al, 2012), although polypharmacological properties of small molecules add complexity to the data interpretation.

Altogether we believe that preclinical efficacy trials in HD mice using small molecules models drug-treatment of human patients reasonably well and are thus applicable for target and therapeutic validation studies. To proceed with the clinical development of a SIRT2 inhibitor for clinical use, it remains imperative to identify structurally diverse SIRT2 inhibitors and to validate the efficacy of these new entities in mouse models of HD and other neurodegenerative diseases.

Experimental Procedure

Animals

Female R6/2 mice used in the study were generated by back-crossing male R6/2 (available from The Jackson Laboratory, Bar Harbor, ME) with C57BL/6 X CBA F1 females. 140CAG knock-in mice were also maintained on B6CBA background. Mice were genotyped by PCR using tail-tip DNA and were housed five per cage under standard conditions with ad libitum access to water and food. To ensure homogeneity of experimental cohorts, mice from the same F generation were systemically assigned to experimental groups such that age, weight, and CAG-repeat lengths were balanced. All animal experiments were carried out in accordance with the National Institutes of Health Guide for the Care and Use of Laboratory Animals and were approved by local animal care committee.

Drug Treatment

Mice were administered different doses of AK-7 (10, 20, and 30 mg/kg) by intraperitoneal injections twice daily starting from 4 weeks of age in both the R6/2 and 140CAG HD mouse models. The drug suspension was made fresh daily. Body weights were recorded weekly at the same time of day. Mice were assessed for morbidity and mortality twice daily. The criterion for euthanasia was the point in time when mice could no longer right themselves within 30 seconds after being placed on their sides. Deaths that occurred overnight were recorded the following morning.

Behavioral Analyses

Motor performance in R6/2 mice was assessed using an accelerating rotarod (Stoelting, Ugo Basile, Biological Research apparatus; Varese, Italy) at 5, 8, and 11 weeks of age. At the beginning of each week, mice were trained for 30 s at a slow speed of 4.5 rpm. Subsequently, three trials were performed for three consecutive days. In each trial, mice were placed onto the rotarod at a constant speed of 4.5 rpm for 5 s, which then accelerated at a constant rate until a terminal angular velocity of 45 rpm was reached. The latency to fall from the rotarod was recorded for each mouse, and the average of three trials was used for statistical analysis. Data were analyzed by using the mixed procedure in SAS version 9.1 software. Results were considered statistically significant at $P < 0.05$.

Behavioral testing for the wild-type and 140CAG mice was performed using open field boxes (Opto-Varimex Unit, Columbus Instruments, OH, USA). Measurements were made for 30 min after 10 min of acclimation to the box. Counts of horizontal and vertical motion activities were monitored and quantitative analysis of locomotor activities (resting and ambulatory times) was assessed. The open-field box was cleaned before testing each mouse. Mice were coded and investigators were blinded to the genotype and analysis. Testing started on week 6 and was performed every other week until the mice could no longer participate.

Histology

At 90 days of age and 6 months, R6/2 and 140CAG mice, respectively, were deeply anesthetized and then transcardially perfused with 2% paraformaldehyde in 0.1M phosphate buffer (pH 7.4). Brains were postfixed with perfusant for 2 days, cryoprotected in a graded series of 10% and 20% glycerol/2% DMSO, and serially sectioned at 50 μm using a SM 2000R freezing microtome (Leica, Wetzlar, Germany). Every eighth section was stained with thionin for striatal volume and neuronal volume analysis. For aggregate immunohistochemistry, floating sections of forebrain at the level of crossing of the anterior commissure were stained with EM48 (dilution, 1:2,000) for 2 days, washed, and incubated with biotinylated secondary antibody and visualized using develope the Vectastain ABC kit (Vector Laboratories, Burlingame, CA). Sections were mounted in aqueous solution (Fluoromount G; Southern Biotech, Birmingham, AL) to prevent *z* axis shrinkage. No signal was detected in the controls in which primary antibody was omitted. Data were analyzed by ANOVA using the GLM procedure in SAS software. Results were considered statistically significant at $P < 0.05$.

Stereology

All analyses were performed blind by using unbiased stereological approaches, Stereo-Investigator software (Micro- BrightField, Williston, VT), and a Leica DMLB microscope with a motorized as described previously (Chopra et al., 2007). Striatal volumes were estimated on every eighth coronal section by using the Cavalieri method. Stereological counts of aggregate number and volumes of cell bodies and intranuclear aggregates were

obtained from the neostriatum at the level of the anterior commissure using the optical fractionator and nucleator methods, respectively. Data were analyzed by ANOVA using the GLM procedure in SAS software. Results were considered statistically significant at $P < 0.05$.

Time-resolved FRET Assay for Soluble Mutant Huntingtin

Brain tissues were homogenized in 10X volume lysis buffer (0.4% Triton X-100 in PBS and 0.1% HALT protease inhibitor) and lysate (5ug/well) were mixed with a reaction buffer (NaH_2PO_4 (50 mM, pH 7.4), NaF (400 mM), BSA (0.1% w/v), and Tween 20, (0.05% v/v) containing fluorophore conjugated antibodies (2B7-Tb, MW1-Alexa 488). The HTRF signal was read on a VICTORX5 plate reader (Perkin Elmer) after 1 h of incubation at 4 °C. After excitation of the Tb donor at 320 nm, emission signals of Alexa488 were detected at 510 nm. The signal resulting from the emission of the Tb was measured at 615 nm and was used for normalization of potential signal artifacts. The 510/615nm ratio values reflect the relative mhtt concentration. Data were analyzed by ANOVA using the GLM procedure in SAS software. Results were considered statistically significant at $P < 0.05$.

Supplementary Material

Refer to Web version on PubMed Central for supplementary material.

Acknowledgments

This study was supported by NIH grant 1U01NS066912-01A1 to AK, SH, RJF, and RBS.

References

The Huntington's Disease Collaborative Research Group. A novel gene containing a trinucleotide repeat that is expanded and unstable on Huntington's disease chromosomes. The Huntington's Disease Collaborative Research Group. Cell. 1993; 72:971–983. [PubMed: 8458085]

Barbaric I, Miller G, Dear TN. Appearances can be deceiving: phenotypes of knockout mice. Brief Funct Genomic Proteomic. 2007; 6:91–103. [PubMed: 17584761]

Beirowski B, Gustin J, Armour SM, Yamamoto H, Viader A, North BJ, Michan S, Baloh RH, Golden JP, Schmidt RE, et al. Sir-two-homolog 2 (Sirt2) modulates peripheral myelination through polarity protein Par-3/atypical protein kinase C (aPKC) signaling. Proc Natl Acad Sci U S A. 2011; 108:E952–961. [PubMed: 21949390]

Bobrowska A, Donmez G, Weiss A, Guarente L, Bates G. SIRT2 ablation has no effect on tubulin acetylation in brain, cholesterol biosynthesis or the progression of Huntington's disease phenotypes in vivo. PLoS One. 2012; 7:e34805. [PubMed: 22511966]

Choi SH, Quinti L, Kazantsev AG, Silverman RB. 3-(N-arylsulfamoyl)benzamides, inhibitors of human sirtuin type 2 (SIRT2). Bioorg Med Chem Lett. 2012; 22:2789–2793. [PubMed: 22446090]

Chopra V, Fox JH, Lieberman G, Dorsey K, Matson W, Waldmeier P, Housman DE, Kazantsev A, Young AB, Hersch S. A small-molecule therapeutic lead for Huntington's disease: preclinical pharmacology and efficacy of C2-8 in the R6/2 transgenic mouse. Proc Natl Acad Sci U S A. 2007; 104:16685–16689. [PubMed: 17925440]

Donmez G, Guarente L. Aging and disease: connections to sirtuins. Aging Cell. 2010; 9:285–290. [PubMed: 20409078]

Hersch SM, Rosas HD. Neuroprotection for Huntington's disease: ready, set, slow. Neurotherapeutics. 2008; 5:226–236. [PubMed: 18394565]

Ji S, Doucette JR, Nazarali AJ. Sirt2 is a novel in vivo downstream target of Nkx2.2 and enhances oligodendroglial cell differentiation. J Mol Cell Biol. 2011; 3:351–359. [PubMed: 21669943]

Jia H, Pallos J, Jacques V, Lau A, Tang B, Cooper A, Syed A, Purcell J, Chen Y, Sharma S, et al. Histone deacetylase (HDAC) inhibitors targeting HDAC3 and HDAC1 ameliorate polyglutamine-

elicited phenotypes in model systems of Huntington's disease. Neurobiol Dis. 2012; 46:351–361. [PubMed: 22590724]

Jia H, Kast RJ, Steffan JS, Thomas EA. Selective histone deacetylase (HDAC) inhibition imparts beneficial effects in Huntington's disease mice: implications for the ubiquitin-proteasomal and autophagy systems. Hum Mol Genet. 2012 Published online September 28 2012.

Luthi-Carter R, Taylor DM, Pallos J, Lambert E, Amore A, Parker A, Moffitt H, Smith DL, Runne H, Gokce O, et al. SIRT2 inhibition achieves neuroprotection by decreasing sterol biosynthesis. Proc Natl Acad Sci U S A. 2010; 107:7927–7932. [PubMed: 20378838]

Maxwell MM, Tomkinson EM, Nobles J, Wizeman JW, Amore AM, Quinti L, Chopra V, Hersch SM, Kazantsev AG. The Sirtuin 2 microtubule deacetylase is an abundant neuronal protein that accumulates in the aging CNS. Hum Mol Genet. 2011; 20:3986–3996. [PubMed: 21791548]

Menalled LB, Sison JD, Dragatsis I, Zeitlin S, Chesselet MF. Time course of early motor and neuropathological anomalies in a knock-in mouse model of Huntington's disease with 140 CAG repeats. J Comp Neurol. 2003; 465:11–26. [PubMed: 12926013]

Moscovitch-Lopatin M, Weiss A, Rosas HD, Ritch J, Doros G, Kegel KB, Difiglia M, Kuhn R, Bilbe G, Paganetti P, et al. Optimization of an HTRF Assay for the Detection of Soluble Mutant Huntingtin in Human Buffy Coats: A Potential Biomarker in Blood for Huntington Disease. PLoS Curr. 2010; 2:RRN1205. [PubMed: 21278900]

Moumne L, Campbell K, Howland D, Ouyang Y, Bates GP. Genetic knockdown of HDAC3 does not modify disease-related phenotypes in a mouse model of Huntington's disease. PLoS One. 2012; 7:e31080. [PubMed: 22347433]

North BJ, Marshall BL, Borra MT, Denu JM, Verdin E. The human Sir2 ortholog, SIRT2, is an NAD +-dependent tubulin deacetylase. Mol Cell. 2003; 11:437–444. [PubMed: 12620231]

Outeiro TF, Kontopoulos E, Altman S, Kufareva I, Strathearn KE, Amore AM, Volk CB, Maxwell MM, Rochet JC, McLean PJ, et al. Sirtuin 2 Inhibitors Rescue {alpha}-Synuclein-Mediated Toxicity in Models of Parkinson's Disease. Science. 2007

Pallos J, Bodai L, Lukacsovich T, Purcell JM, Steffan JS, Thompson LM, Marsh JL. Inhibition of specific HDACs and sirtuins suppresses pathogenesis in a Drosophila model of Huntington's disease. Hum Mol Genet. 2008; 17:3767–3775. [PubMed: 18762557]

Rosas HD, Salat DH, Lee SY, Zaleta AK, Pappu V, Fischl B, Greve D, Hevelone N, Hersch SM. Cerebral cortex and the clinical expression of Huntington's disease: complexity and heterogeneity. Brain. 2008; 131:1057–1068. [PubMed: 18337273]

Stack EC, Kubilus JK, Smith K, Cormier K, Del Signore SJ, Guelin E, Ryu H, Hersch SM, Ferrante RJ. Chronology of behavioral symptoms and neuropathological sequela in R6/2 Huntington's disease transgenic mice. J Comp Neurol. 2005; 490:354–370. [PubMed: 16127709]

Taylor DM, Balabadra U, Xiang Z, Woodman B, Meade S, Amore A, Maxwell MM, Reeves S, Bates GP, Luthi-Carter R, et al. A brain-permeable small molecule reduces neuronal cholesterol by inhibiting activity of sirtuin 2 deacetylase. ACS Chem Biol. 2011; 6:540–546. [PubMed: 21370928]

Truant R, Atwal RS, Desmond C, Munsie L, Tran T. Huntington's disease: revisiting the aggregation hypothesis in polyglutamine neurodegenerative diseases. FEBS J. 2008; 275:4252–4262. [PubMed: 18637947]

Vaquero A, Scher MB, Lee DH, Sutton A, Cheng HL, Alt FW, Serrano L, Sternglanz R, Reinberg D. SirT2 is a histone deacetylase with preference for histone H4 Lys 16 during mitosis. Genes Dev. 2006; 20:1256–1261. [PubMed: 16648462]

Young AB. Huntingtin in health and disease. J Clin Invest. 2003; 111:299–302. [PubMed: 12569151]

Highlights

1. Sirtuin 2 inhibitor is neuroprotective in two HD mouse models
2. SIRT2 inhibitor treatment markedly reduces huntingtin aggregates in HD mouse brain
3. SIRT2 is a promising therapeutic target for neurological protein aggregation disorders

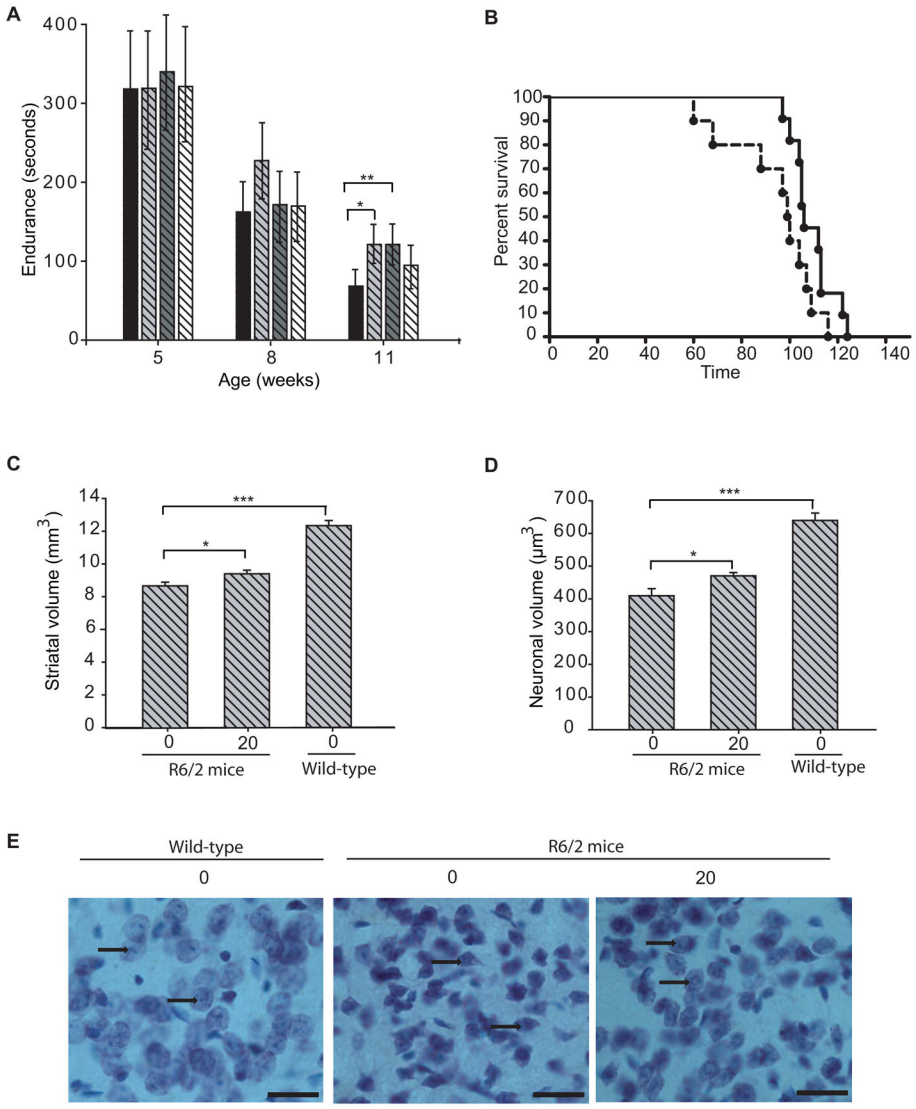

Figure 1. Efficacy of AK-7 in R6/2 mouse model of HD

(A)AK-7 ameliorates motor deficits in HD mice. Latency to fall was increased by 37% at 11 weeks of age (vehicle treated mice = 81s, AK-7 (10mg/kg) treated mice = 129s). Values represent geometric mean ± 95% confidence interval. n = 10–15; * $P \leq 0.05$; **, $P \leq 0.01$ **(B–C)** Kaplein Meier probability of survival analysis (**B**) and the column graph (**C**) shows that AK-7 treatment significantly extends the survival of R6/2 mice by 13.2%; n=10–11. Data is analyzed using Gehan Wilcoxon test with Graph Pad prism (**B**) (p=0. 0.0387) and GLM procedure in SAS software (**C**) (p=0.0280). **(D–E)** Stereological quantification of total striatal volume and neuronal cell body volume. AK-7 treatment (20 mg/kg/12 h) improves the total striatal volume of HD mice by 9% (p = 0.044) and rescues the shrinkage of striatal neuronal cell body volume by 15% (p=0.033). Data represent mean ± SEM, n =8–10; ***, $P \leq 0.001$ **(F)** Thionin-stained sections of neostriatum from a wild-type littermate mouse (*Right*), a placebo-treated R6/2 mouse (*Center*), and an AK-7-treated R6/2 mouse (*Left*) at 12 weeks of age. There is evidence of neuronal atrophy in the untreated R6/2 mouse with relative preservation of neuronal atrophy in the AK-7-treated mouse. The arrowheads represent healthy neurons in Wild-type, shrunken neurons in untreated R6/2 mice, and relatively preserved neurons in AK-7 treated R6/2 mice. (Scale bars, 25 μm.).

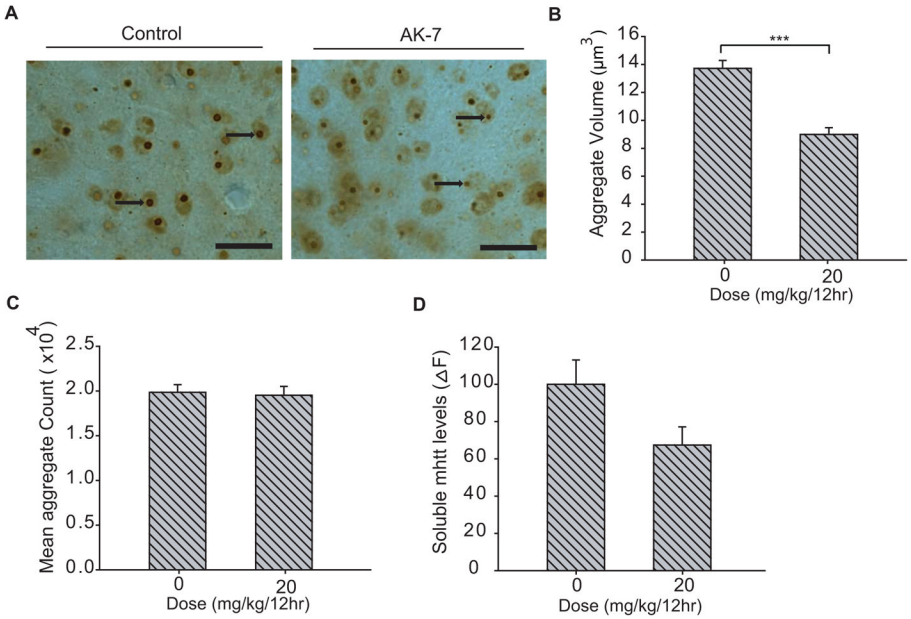

Figure 2. Compound-treatment mediated changes in R6/2 mouse brain

(A) AK-7 decreases the size of striatal neuronal intranuclear huntingtin aggregates. Immunodetection of intraneuronal huntingtin aggregates by using EM48 antibody (arrows) in the neostriatum of 12-week-old R6/2 mice with and without AK-7 treatment (Scale bars, 25 μm.) **(B)** Stereological counts of striatal intraneuronal aggregates in R6/2 mice. AK-7 treatment significantly reduced (35%) the striatal nuclear aggregate volume in R6/2 mice. **(C–D)**AK -7 treatment had no effect on mean aggregate count or levels of soluble mutant huntingtin Exon 1 fragments, as detected by highly sensitive HTRF method. Error bars indicate SEM, ***, $P \leq 0.001$; n=8–10.

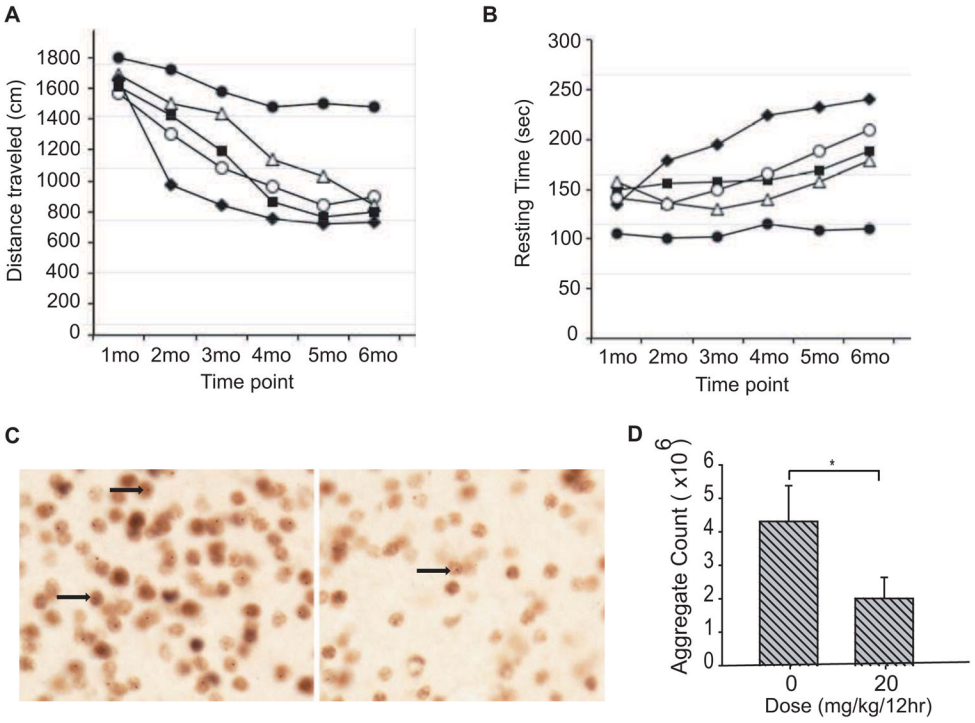

Figure 3. Efficacy of AK-7 in 140CAG knock-in Htt mouse model

A–B) Behavioral test. Open field analysis of AK7 administration in 140CAG mice shows a significant improvement at all the doses in **A**) distance traveled and **B**) resting time, with 20 mg/kg as the most efficacious dose. Symbols: Filled circles = untreated Wild-type, Filled diamond= untreated CAG140, Filled squares=10mg/kg/12h, open triangles=20mg/kg/12h and open circles=30mg/kg/12h. **C**) Aggregation. There was a significant reduction in huntingtin aggregates (untreated 140CAG mice: 4.31 ×106 ± 1.07, AK-7 20mg/kg-treated 140CAG mice: 2.01×106 ± 0.63; $p<0.01$). Arrowheads represent intraneuronal huntingtin aggregates.